5th Joint International Symposium on Deformation Monitoring (JISDM), 20-22 June 2022, Valencia, Spain
DOI: http://doi.org/10.4995/JISDM2022.2022.13863

Evaluation of synthetic aperture radar interferometric techniques for monitoring of fast deformation caused by underground mining exploitation

Kamila Pawłuszek-Filipiak, Maya Ilieva, Natalia Wielgocka, Krzysztof Stasch

Institute of Geodesy and Geoinformatics, Wroclaw University of Environmental and Life Sciences, 50-375 Wrocław, Poland, (kamila.pawluszek-filipiak@upwr.edu.pl; maya.ilieva@upwr.edu.pl; natalia.wielgocka@upwr.edu.pl; krzysztof.stasch@upwr.edu.pl)

Key words: *differential synthetic aperture radar interferometry; small baseline subset; persistent scatterers interferometry; mining*

ABSTRACT

EPOS-PL+ is the Polish national realization of the European Plate Observing System (EPOS) project that aims to build a multidisciplinary infrastructure. It allows integration of a variety of geoscience expertise and techniques to better understand the geohazard related to the underground mining of coal in the Upper Silesian Coal Basin (USCB) in Poland. The study case in this project is the Marcel Mine, located within USCB, where the detected subsidence for the analyzed period of four months reaches 91 cm. Various interferometric processing techniques demonstrated some advantages and also some limitations in the context of mining deformation measurement, including accuracy, spatial resolution, detectable deformation rate, atmospheric delay, and ability to detect the maximal deformation gradients. This is especially important from a mining perspective. Therefore, we investigated three different interferometric processing techniques to monitor fast mining deformation in the Marcel hard coal mine area. More specifically, we used conventional DInSAR, Small Baseline Subsets (SBAS), and Persistent Scattered Interferometry (PSInSAR). The result confirmed that none of these methods can be considered as the best. The DInSAR approach allows capturing the maximal deformation gradient, which was not possible with the PSInSAR and SBAS approaches. On the contrary, PSInSAR and SBAS allow us to provide less noisy and reliable results in the area of safety pillars.

I. INTRODUCTION

Having considered the great potential offered by Synthetic Aperture Radar (SAR) data, within the framework of the European Plate Observing System (EPOS) EPOS-PL+ project, the Satellite Data Infrastructure Center (CIBDS) is established, which aims to build a system to monitor land surface deformation using satellite radar interferometry (Aimaiti *et al*., 2017) from various SAR missions. CIBDS mainly focuses on creating automated algorithms for collecting and processing satellite data, as well as modeling and prediction of land surface deformation. These products will be generated from various SAR sensors (Zhao *et al*., 2019), as well as various interferometric SAR (InSAR) processing techniques (Chang *et al*., 2010) integrated with other geodetic techniques such as leveling, Global Navigation Satellite Systems (GNSS), Light Detection and Ranging (LiDAR) (Froese and Mei, 2008), and photogrammetric techniques (Martins *et al*., 2020). The products generated within CIBDS will be used to assess the risk of severe damage caused by mining activities (Morgan *et al*., 2019) and will be the main source of information necessary to plan future mining works. The main area of monitoring is the safety pillars within the Marcel hard coal mine, located in USCB.

Mining-induced deformation is characterized by high magnitude and nonlinearity and usually leads to serious construction damage (Orwat and Gromysz, 2021). Various interferometric processing techniques demonstrated some advantages and also some limitations in the context of mining deformation measurement, including accuracy, spatial resolution, detectable deformation rate, and atmospheric delay. (Pawluszek-Filipiak and Borkowski 2020; 2021; Zhang *et al*., 2020). Especially from a mining perspective, one of the most important aspects is the estimation of the maximal deformation gradient within the subsiding area. As presented by Ilieva *et al*. (2019); Pawluszek and Borkowski (2021), Differential Synthetic Aperture Radar Interferometry (DInSAR) is shown to be capable of capturing maximal deformation rate. Persistent Scattered Interferometric (PSInSAR) techniques, in addition to their high accuracy, were unable to estimate such a high deformation gradient (Fan *et al*., 2014).

Therefore, the objective of this study was to verify these findings in the Marcel mine area. We investigated three different interferometric processing techniques to monitor rapid mining deformation in the area of the Marcel hard coal mine. More specifically, we used conventional DInSAR, Small Baseline Subsets (SBAS) proposed by Berardino *et al*. (2002), and Persistent Scattered Interferometry (PSInSAR) proposed by Ferretti *et al*. (2000). Evaluation of these techniques has been carried out on Sentinel-1 data.

II. Study Area

The study area of the Marcel mine is located in USCB, one of the largest hard coal mining areas in Europe. The largest part of USCB is located in Poland, and the remainder lies in the Czech Republic. Within USCB many active hard coal mines are located. The ‘Marcel’ mine (until 1949, the mine was called ‘Emma’) dates back to the mid-19th century. The mine was fully launched on November 13, 1883. Construction of the mine took 10 years. Currently, the mine employs 3,168 people and its daily net hard coal production is 11,000 tons (Dreger, 2019).

Figure 1 presents the location of the safety pillars within the ‘Marcel’ mine, which are the main objective of the deformation monitoring in this area. The investigated study covers 25 km^2 and ranges from 18°29‘0”E to 13°33‘0”E in longitude and from 50°1’0”N up to 50°3’0”N in latitude. As can be seen in Figure 1, the study area is mainly covered by agricultural areas with sparse buildings, which means that the number of persistent natural scatters will be limited. Therefore, the application of distributed scatters (DS) seems to provide a better information of the spatial coverage of (Sun *et al.*, 2018).

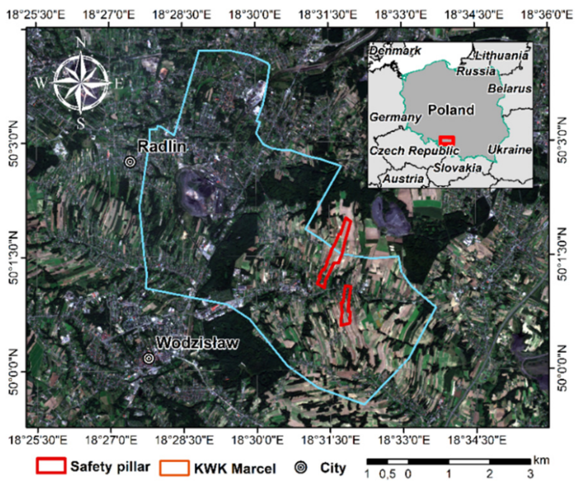

Figure 1. Location of the safety pillars within the study area of Marcel mine.

III. Methodology

The overall methodology applied in this study is presented in Figure 2. The ascending and descending SAR dataset captured from the Sentinel Open Access Hub, as well as from Alaska Satellite Facility were used. The location of the safety pillars with the Marcel mine was also provided by the Polish Mining Group within the EPOS-PL+ project. For InSAR processing European Space Agency (ESA) SNAP and SARScape® software were used. Cumulated deformation maps for the last four months of 2020 were used to create deformation profiles and make a comparison of these methods.

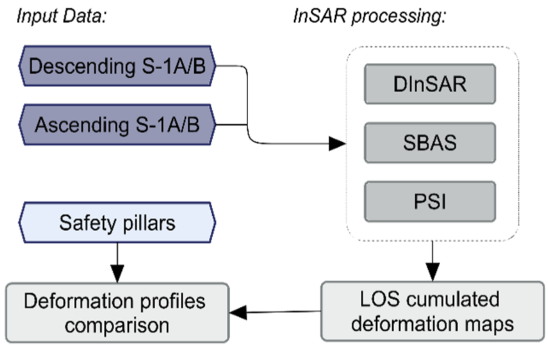

Figure 2. Methodology utilized in this study.

A. *Data used*

In the presented study, we used only SAR data of the C-band (~5.55 cm wavelength) of the ESA Sentinel-1A/B satellites, which are freely available online on the ESA’s Copernicus Sentinel data hub.

The chosen data are acquired in Interferometric Wide Swath (IW) mode of ascending and descending geometry, in Single Look Complex (SLC) format, and cover the time period between last four months of the year 2020; more specifically, ascending data cover the period from 3th of September 2020 up to 26th of December 2020 while ascending data cover the period from 26th of August up to 5th of January. Having considered the dense vegetation cover in the study area, the investigated period was shortened into the time span of approximately 4 months. This allows to mitigate the effect of the decorrelation and to collect more information in the vegetated areas. Table 1 presents the specific characteristics of the data used in this study.

Table 1. Specification of the data used

	Ascending S-1A/B	Descending S-1A/B
Number of images	20	21
Period	2020/09/03 - 2020/12/26	2020/08/26 - 2021/01/05
Mean Incidence Angle [°]	38.3	43.7
Mean Azimuth [°]	81.7	-78.9
Relative Orbit	175	51
Mode	IW	IW

B. *Interferometric processing*

As mentioned previously, the study area is mostly agricultural and thus the number of coherent areas with stable backscattering signal will be low. Since the CIBDS aim to effectively monitor safety pillars within the Marcel mine, the high density and accuracy of the measurement are beneficial. Therefore, various SAR sensors as well as various interferometric processing techniques should be evaluated in this context to provide higher density and precision. In the literature, there are many diverse interferometric processing methods, but we decided to apply and compare three techniques, namely conventional consecutive DInSAR, SBAS, and PSInSAR. The PSInSAR and SBAS processing was performed with SARScape software (Sahraoui *et al.*, 2006), while the consecutive DInSAR approach was applied using the ESA Sentinel Application Platform (SNAP).

The data set described in Table 1 was processed as separate DInSAR interferograms, formed by 6-day pairs of consecutive Sentinel-1 images to minimize the temporal decorrelation considering the land cover of the area of interest. The Shuttle Radar Topography Mission (SRTM) 1 arc second (30 m resolution) Digital Elevation Model (DEM) was applied for topographic phase removal. Goldstein filters (Goldstein and Werner, 1998) are applied to the received wrapped interferograms, aiming to reduce the noise and to support the unwrapping of the radar phases. The minimum cost flow (MCF) function was used for phase unwrapping (Chen and Zebker, 2000). In all processing steps, a threshold of 0.3 for the pixel coherence was used, while the final results are interpolated and resampled to 20 m pixel spacing. A selection of forest features from the CORINE Land Cover (version 2018) (© European Union, 2018) inventory was applied to exclude densely vegetated areas with extremely low coherence. By combining consecutive interferograms, the total amount of the subsidence in the area of investigation is retrieved with some of the atmospheric artifacts also canceled out.

More advanced DInSAR processing involves the SBAS method, which presents a key advantage compared with other interferometric processing methods (Berardino *et al*., 2002). SBAS generates interferograms from appropriately selected pairs of SAR images to minimize the spatial and temporal baseline between two images in the pairs. In the presented study, normal baseline constraints were set at 2% of the critical baseline. Additionally, the maximum temporal baseline constraint was set to 30 days for both SBAS processing steps (in ascending and descending orbits). This allows us to mitigate the decorrelation problem that occurs with longer baselines. Generally, SBAS estimates various interferometric components (deformation, atmosphere, and other components) and provides almost error-free results (Iglesias *et al*., 2015). SBAS takes advantage of the interferogram redundancy and estimates deformation using singular value decomposition. The atmospheric phase screen (APS) is estimated by using high-pass and low-pass filtering of the phase. In addition, the quadratic deformation model was used to estimate various interferometric components. The MCF function with 0.4 coherence threshold was used for phase unwrapping.

The third technique in the current comparison is the PSInSAR method that allows one to identify most coherent points with high resolution and with high spatial density (Ferretti, 2000; 2001). However, to properly estimate all interferometric components, in this approach a linear deformation model in time is adopted within InSAR processing. Therefore, PS points that have strongly nonlinear deformation behavior in time will not be selected as PS candidates since they did not meet the model fitting criteria (temporal coherence is low). Therefore, estimating the maximal deformation gradient using these techniques is very often a challenge. However, from another point of view, phase unwrapping is carried out in the spare grid; therefore, the probability of phase jumps errors which are very probable to occur in noncoherent areas using spatial phase unwrapping is lower.

It is worth mentioning that in literature there are also other PSInSAR methods which did not apply linear deformation models in processing. For instance, StaMPS (Stanford Method for Persistent Scatterers) utilizes spatial correlation method which is dedicated to the vegetated areas (Hooper *et al*., 2007; Delgado 2019).

IV. Results

Figure 3 presents InSAR processing results using different techniques: PSInSAR in the upper row (a and b), SBAS in the middle row (c and d) and DInSAR in the lower row (e and f), with ascending results to the left (a, c, and e) and descending to the right (b, d, and f). As can be observed, in general the results are similar to each other but severe differences occur. However, the results of PSInSAR did not allow us to estimate deformation with a fast gradient. The maximum deformation estimated using PSInSAR for the ascending and descending orbits is not greater than 20 cm. Nevertheless, it can be observed that stable areas are represented as green and that values oscillate around zero. Furthermore, processing using the SBAS technique allows us to effectively estimate fast deformation in the center of the subsidence bowls, as well as accurate estimation of the deformation within the stable areas. It was possible to capture the maximum deformation gradient for ascending and descending images of -48 cm and -39 cm, respectively.

Moreover, observing results from DInSAR processing, it can be noted that the maximal deformation gradient for one of the detected subsidence basins is 91 cm and 87 cm for ascending and descending orbits. Therefore, it indicated that none of the multi-temporal interferometric processing techniques such as PSInSAR or SBAS allow us to capture the full deformation gradient. Nevertheless, observing results in stable areas, it can be seen that more noisy pixels exist, especially for the results of descending orbit. One of the reasons could be the presence of some atmospheric artifacts that were not fully modeled and subtracted from the DInSAR results. To better understand the advantages and limitations of each technique, deformation profiles were generated and presented in Figure 4. These deformation profiles were extracted from areas with the highest deformation gradient detected as well as from two safety pillars. As can be observed, the maximal deformation gradient was detected in various locations for ascending and descending geometry. This probably indicates that significant horizontal deformation exists within the investigated area. Many previous works demonstrated that considerable horizontal movement (approximately 30-40% of the maximal vertical gradient) exists on the edges of the subsidence bowls caused by underground coal excavation (Li *et al*., 2015; Pawluszek-Filipiak and Borkowski 2020).

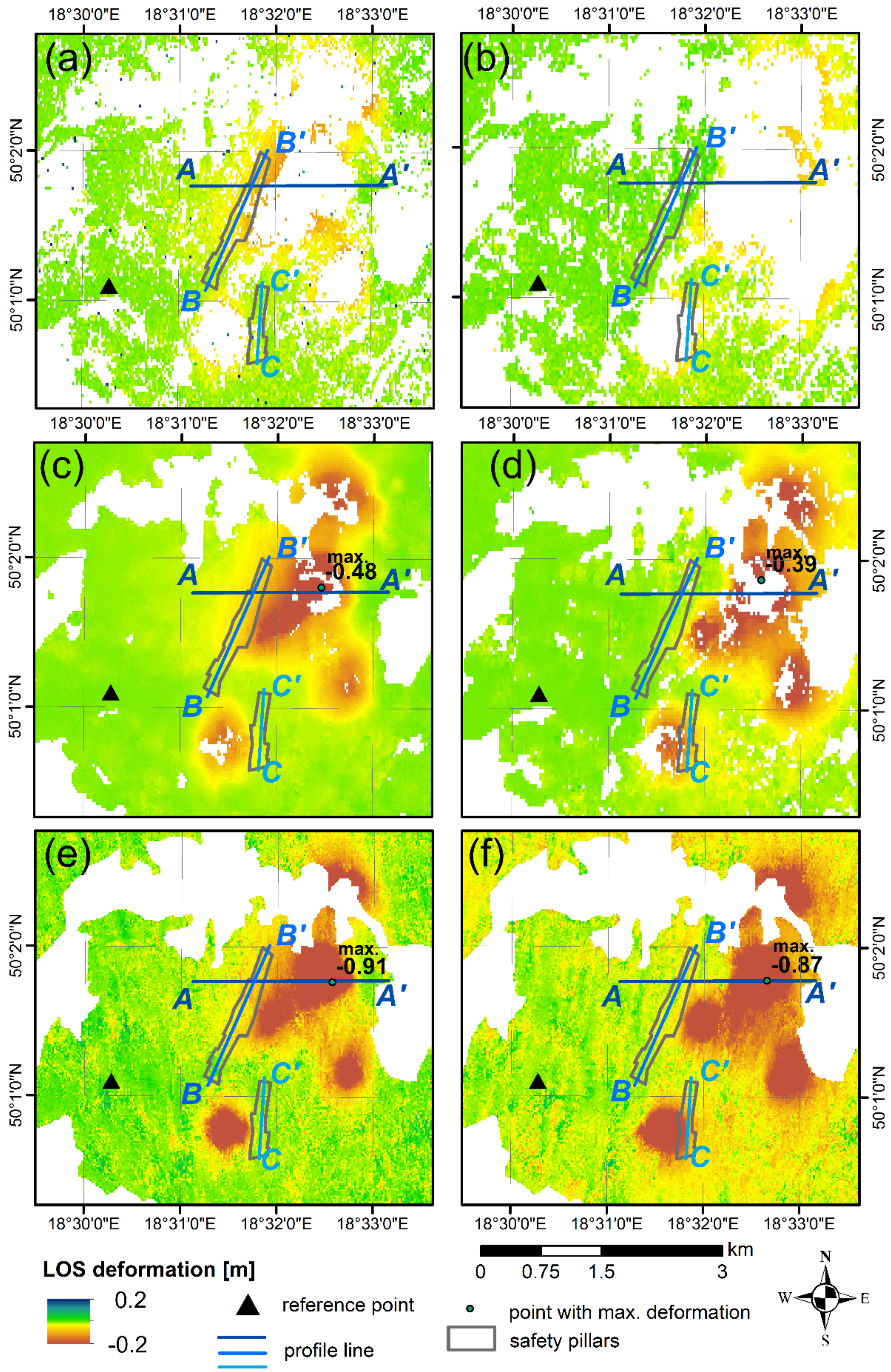

Figure 3. InSAR results using different processing techniques: PSInSAR (a, b), SBAS (c, d) and DInSAR (e,f) from ascending (a, c, and e) and descending (b, d, and f) geometries.

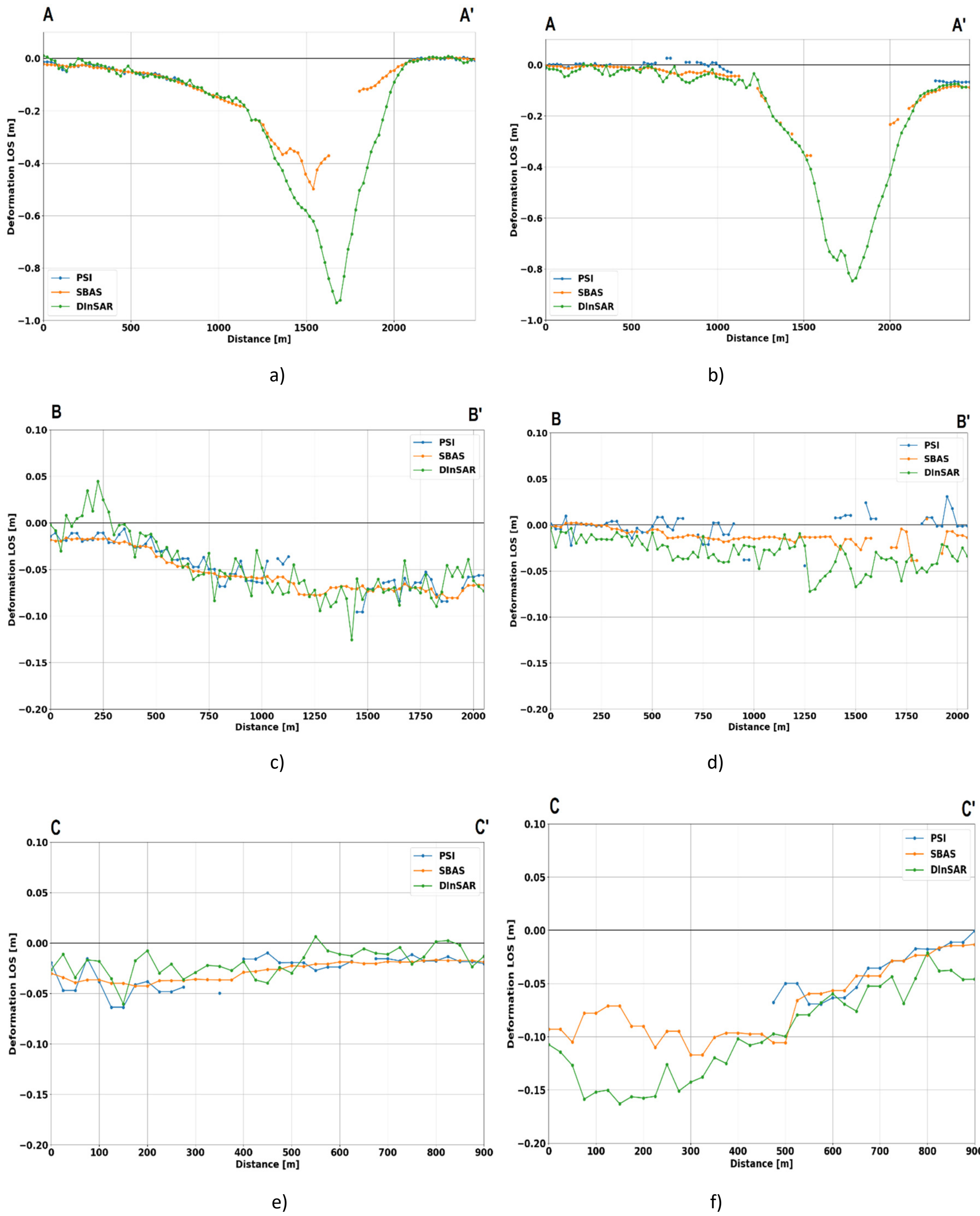

Figure 4. Deformation profiles across the area of maximum detected deformation for ascending (a) and descending (b), for first safety pillar from ascending (a) and descending (d) and second safety pillar for ascending (e) and descending orbit (f).

Additionally, for ascending geometry, it is visible that the SBAS method underestimated the deformation gradient. Since the atmospheric effect is assumed to be similar for the surrounding pixels, the incompatibility between DInSAR and SBAS rather corresponds to phase unwrapping errors in the SBAS results. Moreover, for the descending orbit (Figure 4a), some disagreement between DInSAR and SBAS results exists in the profile distance 1600-1620m. This can contribute to some interferometric processing errors in one of the applied methods (such as phase jumps or phase aliasing problems in SBAS results or atmospheric effect in DInSAR results). Unfortunately, by the preparation of this report we did not have ground-truth geodetic measurements for comparison and evaluation of the accuracy of the delivered products.

Observing the results for the profiles extracted for the areas where safety pillars are located, it can be observed that in this case the PSInSAR and SBAS results are more smooth for both profiles (BB') and (CC'). However, it can be observed that the smoothest results are present for SBAS products. The PSInSAR processing results are interrupted due to the lower number of PS points.

V. Discussion

The comparison of the three InSAR processing techniques evaluated indicated that each of them provide different results in terms of maximum detected deformation, density of the points. Meeting all criteria for the effective monitoring of mining areas such as high accuracy, high measurement point density, and capability to capture maximal deformation gradient is very challenging. As observed, the DInSAR approach allows to capture maximal deformation gradients which was not possible with the PSInSAR and SBAS approaches. In contrast, PSInSAR and SBAS allow us to provide less noisy and reliable results in the area of safety pillars.

Additionally, PSInSAR due to the high constraints imposed on coherence (0.7) amplitude dispersion (0.25) and deformation model in time provide less measurement points which affect understanding of the partial behavior of the subsidence basin. Moreover, considering the constraints about the minimum number of SAR images, the PSInSAR method is the most critical since in this case at least 20 images are needed to correctly evaluate interferometric components.

VI. Conclusions and future work

Interferometric techniques are shown to be a powerful tool for monitoring mining deformation. Unfortunately, the high deformation gradient experience in that study (0.9 m / 4 month) indicated that more targeted solutions must be prepared to accurately measure the mining deformation from space and, at the same time, provide the highest possible accuracy.

The result in this study demonstrated that each of the interferometric techniques has its own advantages and limitations in the context of high accuracy, high measurement point density, and the capabilities to capture the maximal deformation gradient of the mining subsidence bowls.

Therefore, in the future we will try to tailor InSAR processing towards these critical aspects and the proposed integrated and complex approach of monitoring mining deformations. The products will be evaluated based on ground-truth data which we have already started to capture. More specifically, we located more than 250 stable points along more than 18 kilometers of roads in the Marcel mine area. We are planning ground-truth measurements in six-month intervals. The first one was already performed in the fourth quarter of 2021, which includes leveling, total station, and satellite measurements of the Global National Satellite System (GNSS). The control points located on the safety pillars are connected to GNSS permanent stations, located outside of the deformation zone.

Also, in the future work the application of L- band data from ALOS-2 mission will be evaluated in the context of accuracy and ability to capture such a high deformation gradient in non-coherent vegetated areas to mitigate the mining needs.

VII. Acknowledgements

The research infrastructure that has been used for computation purposes was created within the project EPOS-PL (POIR.04.02.00-14-A003/16) and EPOS-PL+ (POIR.04.02.00-00-C005/19-00) European Plate Observing System, funded by the Operational Programme Smart Growth 2014–2020, Priority IV: Increasing the research potential, Action 4.2: Development of modern research infrastructure of the science sector and co-financed by the European Regional Development Fund. Kamila Pawluszek-Filipiak is supported by the Ministry of Science and Education in the framework of Scholarship for the best young scientists (SMN/16/1429/2020)

References

© European Union, (2018). Copernicus Land Monitoring Service European Environment Agency (EEA), https://land.copernicus.eu/pan-european/corine-land-cover/clc2018

Aimaiti, Y., Yamazaki, F., Liu, W., and Kasimu, A. (2017). Monitoring of land-surface deformation in the karamay oilfield, Xinjiang, China, using sar interferometry. *Applied Sciences*, 7(8), 772. DOI: 10.3390/app7080772

Berardino, P., Fornaro, G., Lanari, R., and Sansosti, E. (2002). A new algorithm for surface deformation monitoring based on small baseline differential SAR interferograms. *IEEE Transactions on geoscience and remote sensing*, 40(11), 2375-2383, DOI: 10.1109/TGRS.2002.803792

Chang, C. P., Yen, J. Y., Hooper, A., Chou, F. M., Chen, Y. A., Hou, C. S., and Lin, M. S. (2010). Monitoring of Surface Deformation in Northern Taiwan Using DInSAR and PSInSAR Techniques. *Terrestrial, Atmospheric & Oceanic Sciences*, 21(3). DOI: 10.3319/TAO.2009.11.20.01(TH)

Chen, C.W. and Zebker, H.A. (2000). Network approaches to two-dimensional phase unwrapping: Intractability and two new algorithms. *Journal of the Optical Society of America* A, 17(3), 401-414, DOI: 10.1364/JOSAA.17.000401

Delgado Blasco, J. M., Foumelis, M., Stewart, C., and Hooper, A. (2019). Measuring urban subsidence in the Rome metropolitan area (Italy) with Sentinel-1 SNAP-StaMPS persistent scatterer interferometry. *Remote Sensing*, 11(2), 129.

Dreger, M. (2019). Methane emissions in selected hard-coal mines of the Upper Silesian Coal Basin in 1997–2016. *Geology, Geophysics and Environment*, 45(2). DOI: 10.7494/geol.2019.45.2.121

Fan, H. D., Wei, G., Yong, Q., Xue, J. Q., and Chen, B. Q. (2014). A model for extracting large deformation mining subsidence using D-InSAR technique and probability integral method. *Transactions of Nonferrous Metals Society of China*, 24(4), 1242-1247. DOI: 10.3390/rs11070812

Ferretti, A., Prati, C., and Rocca, F. (2000). Nonlinear subsidence rate estimation using permanent scatterers in differential SAR interferometry. *IEEE Transactions on geoscience and remote sensing*, 38(5), 2202-2212, DOI: 10.1109/36.868878

Ferretti, A., Prati, C., and Rocca, F. (2001). Permanent scatterers in SAR interferometry. *IEEE Transactions on geoscience and remote sensing*, 39(1), 8-20, DOI: 10.1109/36.898661

Froese, C. R., and Mei, S. (2008). Mapping and monitoring coal mine subsidence using LiDAR and InSAR. *GeoEdmonton*, 8, 1127-1133. DOI: 10.34218/IJCIET.11.6.2020.003

Goldstein, R. M. and Werner, C. L. (1998). Radar interferogram filtering for geophysical applications. *Geophysical Journal International*, 25(21), pp. 4035-4038, DOI: 10.1029/1998GL900033

Hooper, A., Segall, P., and Zebker, H. (2007). Persistent scatterer interferometric synthetic aperture radar for crustal deformation analysis, with application to Volcán Alcedo, Galápagos. *Journal of Geophysical Research: Solid Earth*, 112(B7).

Iglesias, R., Mallorqui, J. J., Monells, D., López-Martínez, C., Fabregas, X., Aguasca, A., and Corominas, J. (2015). PSI deformation map retrieval by means of temporal sublook coherence on reduced sets of SAR images. *Remote Sensing*, 7(1), 530-563. DOI: 10.3390/rs70100530

Ilieva, M., Polanin, P., Borkowski, A., Gruchlik, P., Smolak, K., Kowalski, A., Rohm, W. (2019). Mining Deformation Life Cycle in the Light of InSAR and Deformation Models. *Remote Sensing*, 11, 745. DOI:10.3390/rs11070745

Li, Z. W., Yang, Z. F., Zhu, J. J., Hu, J., Wang, Y. J., Li, P. X., and Chen, G. L. (2015). Retrieving three-dimensional displacement fields of mining areas from a single InSAR pair. *Journal of Geodesy*, 89(1), pp. 17-32. DOI: 10.1007/s00190-014-0757-1

Martins, B. H., Suzuki, M., Yastika, P. E., and Shimizu, N. (2020). Ground Surface Deformation Detection in Complex Landslide Area—Bobonaro, Timor-Leste—Using SBAS DInSAR, UAV Photogrammetry, and Field Observations. *Geosciences*, 10(6), 245. DOI: 10.3390/geosciences10060245

Morgan, J. L., Colombo, D., and Meloni, F. (2019, April). InSAR tools for risk assessment over mine assets. In Proceedings of the First International Conference on Mining Geomechanical Risk (pp. 159-170). Australian Centre for Geomechanics. DOI: 10.36487/ACG_rep/1905_06_Morgan

Orwat, J., and Gromysz, K. (2021, February). Occurrence consequences of mining terrain surface discontinuous linear deformations in a residential building. In *Journal of Physics: Conference Series* (Vol. 1781, No. 1, p. 012013). IOP Publishing, DOI: 10.1088/1742-6596/1781/1/012013

Pawluszek-Filipiak, K., and Borkowski, A. (2020). Integration of DInSAR and SBAS Techniques to determine mining-related deformations using sentinel-1 data: The case study of Rydułtowy mine in Poland. *Remote Sensing*, 12(2), 242. DOI: 10.3390/rs12020242

Pawluszek-Filipiak, K., and Borkowski, A. (2021). Monitoring mining-induced subsidence by integrating differential radar interferometry and persistent scatterer techniques. European Journal of Remote Sensing, 54(sup1), pp. 18-30, DOI: 10.1080/22797254.2020.1759455

Sahraoui, O. H., Hassaine, B., Serief, C., and Hasni, K. (2006). Radar interferometry with Sarscape software. *Photogrammetry and Remote Sensing*.

SNAP, ESA (2021). Sentinel Application Platform v8.0.0, http://step.esa.int

Sun, Q., Jiang, L., Jiang, M., Lin, H., Ma, P., and Wang, H. (2018). Monitoring coastal reclamation subsidence in Hong Kong with distributed scatterer interferometry. *Remote Sensing*, 10(11), 1738. DOI: 10.3390/rs10111738

Zhang, L., Cai, X., Wang, Y., Wei, W., Liu, B., Jia, S., ... and Wei, Z. (2020). Long-term ground multi-level deformation fusion and analysis based on a combination of deformation prior fusion model and OTD-InSAR for longwall mining activity. *Measurement*, 161, 107911, DOI: 10.1016/j.measurement.2020.107911

Zhao, Q., Ma, G., Wang, Q., Yang, T., Liu, M., Gao, W., ... and Pepe, A. (2019). Generation of long-term InSAR ground displacement time-series through a novel multi-sensor data merging technique: The case study of the Shanghai coastal area. *ISPRS Journal of Photogrammetry and Remote Sensing*, 154, pp. 10-27. DOI: 10.1016/j.isprsjprs.2019.05.005